

Self-supervised Conformal Prediction for Uncertainty Quantification in Imaging Problems

Jasper M. Everink¹[0000-0001-7263-0317], Bernardin Tamo Amougou^{2,3}, and
Marcelo Pereyra²[0000-0001-6438-6772]

¹ Technical University of Denmark, Kgs. Lyngby, Denmark, jmev@dtu.dk

² Heriot-Watt University & Maxwell Institute for Mathematical Sciences, Edinburgh,
UK

³ Université de Paris Cité, Paris, France

Abstract. Most image restoration problems are ill-conditioned or ill-posed and hence involve significant uncertainty. Quantifying this uncertainty is crucial for reliably interpreting experimental results, particularly when reconstructed images inform critical decisions and science. However, most existing image restoration methods either fail to quantify uncertainty or provide estimates that are highly inaccurate. Conformal prediction has recently emerged as a flexible framework to equip any estimator with uncertainty quantification capabilities that, by construction, have nearly exact marginal coverage. To achieve this, conformal prediction relies on abundant ground truth data for calibration. However, in image restoration problems, reliable ground truth data is often expensive or not possible to acquire. Also, reliance on ground truth data can introduce large biases in situations of distribution shift between calibration and deployment. This paper seeks to develop a more robust approach to conformal prediction for image restoration problems by proposing a self-supervised conformal prediction method that leverages Stein’s Unbiased Risk Estimator (SURE) to self-calibrate itself directly from the observed noisy measurements, bypassing the need for ground truth. The method is suitable for any linear imaging inverse problem that is ill-conditioned, and it is especially powerful when used with modern self-supervised image restoration techniques that can also be trained directly from measurement data. The proposed approach is demonstrated through numerical experiments on image denoising and deblurring, where it delivers results that are remarkably accurate and comparable to those obtained by supervised conformal prediction with ground truth data.

Keywords: Conformal Prediction · High-Dimensional Image Restoration Problems · Stein’s Unbiased Risk Estimate.

1 Introduction

Image restoration tasks often carry a significant amount of uncertainty, as they admit a wide variety of solutions that are equally in agreement with the observed data. Quantifying and characterizing this uncertainty is important for

applications that depend on restored images to inform critical decisions. Several statistical frameworks exist to address uncertainty quantification (UQ) in imaging sciences. Among these, the Bayesian statistical framework has been extensively studied and applied [1], enabling the incorporation of prior knowledge and providing probabilistic interpretations of uncertainty. This framework supports a diverse range of modeling and algorithmic approaches, as demonstrated in works such as [2, 3, 4, 5]. Unfortunately, despite significant progress in the field, state-of-the-art Bayesian imaging methods are not yet able to provide accurate UQ on structures that are larger than a few pixels in size [6].

With regards to non-Bayesian approaches to UQ in image restoration, the recently proposed equivariant bootstrapping method [7] offers excellent frequentist accuracy, even for large image structures. This is achieved by exploiting known symmetries in the problem to reduce the bias inherent to bootstrapping. Equivariant bootstrapping is particularly accurate in problems that are highly ill-posed, such as compressive sensing, inpainting and limited angle tomography and radio-interferometry, as in these cases the bias from bootstrapping is almost fully removed by the actions of the symmetry group [7, 8]. Conversely, equivariant bootstrapping struggles with problems that are not ill-posed, such as image denoising or mild deblurring, as in this case it is difficult to identify symmetries to remove the bias from bootstrapping (see [7] for details).

Moreover, when sufficient ground truth data are available for calibration, conformal prediction presents another highly flexible strategy for UQ in image restoration. Crucially, conformal prediction can be seamlessly applied to any image restoration technique to deliver UQ results that, by construction, have nearly exact marginal coverage [9]. Also, conformal prediction can be easily combined with other UQ strategies, such as Bayesian imaging strategies (see, e.g., [10]) or equivariant bootstrapping [8], as a correction step.

However, as mentioned previously, in its original form, conformal prediction approaches require access to abundant ground truth data for calibration. In many applications, access to ground truth data is either expensive or impossible. Also, reliance on ground truth data for calibration can lead to poor accuracy in situations of distribution shift between calibration and deployment. To address this limitation of conformal prediction, we propose a self-supervised conformal prediction method that leverages Stein’s Unbiased Risk Estimator (SURE) to self-calibrate UQ results directly from the observed noisy measurements, bypassing the need for ground truth.

The remainder of this paper is organized as follows. Section 2 provides an overview of conformal prediction and a formal problem statement. Section 3 introduces the proposed self-supervised conformal prediction method. Section 4 demonstrates the proposed approach through numerical experiments on image denoising and non-blind deblurring tasks and by considering model-based as well as learning-based estimators. Conclusions and perspectives for future work are finally reported in Section 5.

2 Problem statement

We consider the estimation of a set of plausible values for an unknown image of interest $x^* \in \mathbb{R}^n$, from a noisy degraded measurement $y \in \mathbb{R}^m$. We assume that x^* is a realization of a random variable X , and y is a realization of the conditional random variable $Y|X = x^*$. A point estimator for x^* , derived from Y , is henceforth denoted by $\hat{x}(Y)$. We focus on the case where observations follow a Gaussian noise model:

$$(Y|X = x^*) \sim \mathcal{N}(Ax^*, \sigma^2 \mathbb{I}_m),$$

where $A \in \mathbb{R}^{m \times n}$ models deterministic instrumental aspects of the image restoration problem, $\sigma^2 > 0$ is the noise variance, and \mathbb{I}_m is the $m \times m$ identity matrix. Throughout the paper we assume A is a full-rank but potentially highly ill-conditioned linear operator.

Our goal is to construct a region $C(Y) \subset \mathbb{R}^n$ in the solution space such that

$$\mathbb{P}_{(X,Y)}(X \in C(Y)) \geq 1 - \alpha, \quad (1)$$

where the probability is taken with respect to the joint distribution of (X, Y) , and $\alpha \in [0, 1]$ specifies the desired confidence level.

To illustrate, suppose that x^* is a high-resolution MRI scan of an adult brain. The random variable X characterizes the distribution of brain MRI scans for a generic individual within the population, as obtained by an ideal noise-free and resolution-perfect MRI scanner. The specific image x^* corresponds to an MRI scan of a particular individual, while y represents the noisy, degraded measurement acquired in practice. The estimator $\hat{x}(y)$ produces an estimate of x^* . The region $C(y)$ encapsulates a set of plausible solutions, rather than a single estimate, and satisfies the guarantee in (1). This means that if the procedure is repeated across a large number of individuals from the population, the constructed regions C will contain the respective true images x^* in at least $1 - \alpha$ of the cases.

Conformal prediction provides a general framework for constructing sets C with the desired probabilistic guarantee [9]. This is achieved using a *non-conformity measure* $s : \mathbb{R}^n \times \mathbb{R}^m \rightarrow \mathbb{R}$. By computing the top $(1 - \alpha)$ -quantile q_α of the statistic $s(X, Y)$, the set $C(y)$ is defined as:

$$C(y) := \{x \in \mathbb{R}^n \mid s(x, y) \leq q_\alpha\} \quad \text{for all } y \in \mathbb{R}^m.$$

By construction, this set satisfies:

$$\mathbb{P}_{(X,Y)}(X \in C(Y)) = \mathbb{P}_{(X,Y)}(s(X, Y) \leq q_\alpha) \geq 1 - \alpha,$$

for any confidence level $\alpha \in (0, 1)$. With a sufficiently large sample $\{x_i, y_i\}_{i=1}^M$ to calibrate q_α , any suitable function s can be used to construct a set C that contains x^* with high probability under the joint distribution of (X, Y) .

A popular specific implementation of this framework is *split conformal prediction*. Given a training sample $\{X_i, Y_i\}_{i=1}^M$ of independent (or exchangeable)

realizations of (X, Y) , the method estimates the top $\frac{\lceil (M+1)(1-\alpha) \rceil}{M}$ -quantile \hat{Q}_α of $\{s(X_i, Y_i)\}_{i=1}^M$. For a new observation $(X_{\text{new}}, Y_{\text{new}})$, the prediction set is then:

$$\hat{C}(Y_{\text{new}}) := \{X_{\text{new}} \in \mathbb{R}^n \mid s(X_{\text{new}}, Y_{\text{new}}) \leq \hat{Q}_\alpha\}.$$

This set satisfies the guarantee:

$$\mathbb{P}_{(X, Y)^{M+1}} \left(X_{\text{new}} \in \hat{C}(Y_{\text{new}}) \right) \geq 1 - \alpha, \quad (2)$$

where the probability accounts for the joint distribution of the M training samples and the new observation. Notably, this formulation includes a finite-sample correction because \hat{Q}_α is derived from the $\frac{\lceil (M+1)(1-\alpha) \rceil}{M}$ -quantile. This correction becomes negligible as $M \rightarrow \infty$. For an excellent introduction to conformal prediction, please see [9].

While the conformal prediction framework is highly flexible, not all non-conformity measures $s(x, y)$ deliver prediction regions that are equally useful in practice. Indeed, all prediction sets $\hat{C}(y)$ take the form of a sub-level set of the function $x \mapsto s(x, y)$, which can be arbitrarily chosen. As a result, it is possible to construct infinitely many regions in \mathbb{R}^n that satisfy the guarantee of containing the true solution x^* with probability at least $1 - \alpha$. However, many of these regions may be excessively large, especially in high-dimensional settings, where poorly designed score functions $s(x, y)$ can lead to regions $\hat{C}(y)$ that are overly conservative and cover most of the support of X .

Carefully designing $s(x, y)$ allows obtaining conformal prediction sets that are compact and informative, even in high dimension. In particular, it is essential that $s(x, y)$ is constructed in a way that reduces the variability of $s(X, Y)$. Of particular interest are normalized non-conformity measures of the form [11]:

$$s(x, y) = \|x - \hat{x}(y)\|_{\Sigma(y)}^2 = (x - \hat{x}(y))^\top \Sigma(y) (x - \hat{x}(y)), \quad (3)$$

where $\Sigma(y)$ is a positive definite matrix of size $n \times n$. A well-chosen $\Sigma(y)$ reduces variability in $s(X, Y)$, leading to prediction sets that are well-centered around $\hat{x}(y)$, compact, and highly informative. In practice, $\Sigma(y)$ is often chosen as an approximation of the inverse-covariance matrix of the error $X - \hat{x}(Y)$ [11].

A fundamental obstacle to applying conformal prediction to image restoration problems is the need for paired samples $\{x_i, y_i\}$, as obtaining the ground truth image x_i is precisely the goal of solving the imaging problem in the first place. This can be partially mitigated by relying on a training dataset, at the risk of delivering poor results in situations of distribution shift (e.g., returning to our illustrative example related to MRI imaging, when the population encountered in deployment differs significantly from the population used for calibration). In this paper, we propose a greatly more robust and deployable approach to conformal prediction that relies solely on the observed measurements $\{y_i\}_{i=1}^M$.

3 Proposed Method

Our proposed self-supervised conformal prediction method circumvents the need for ground truth data by leveraging Stein’s unbiased risk estimate (SURE) [12].

We begin by pooling together M exchangeable imaging problems, where each problem involves an unknown image x_i^* and an observation y_i which we consider to be a realisation of the conditional random variable $(Y|X = x_i^*) \sim \mathcal{N}(Ax_i^*, \sigma^2 \mathbb{I}_m)$. To specify the non-conformity measure, we consider $\Sigma(y) = A^\top A$ which is a natural choice for approximation for the error inverse-covariance when $(Y|X = x_i^*) \sim \mathcal{N}(Ax_i^*, \sigma^2 \mathbb{I}_m)$, as we expect $\hat{x}(Y)$ to be accurate along the leading eigenvectors of $A^\top A$ and the estimation error to concentrate along weak eigenvectors of $A^\top A$. This leads to the non-conformity measure

$$s(x, y) = \frac{1}{m} \|Ax - A\hat{x}(y)\|_2^2, \tag{4}$$

where we recall that A is assumed full-rank, but potentially very poorly conditioned. We require A to be full rank as otherwise $\Sigma(y)$ is only positive semidefinite, implying that the corresponding prediction set can be unbounded.

To calibrate without ground truth data, instead of relying on a sample quantile of $\{s(x_i, y_i)\}_{i=1}^M$, we rely on SURE to provide unbiased estimates of $\{s(x_i, y_i)\}_{i=1}^M$ from the observed measurements $\{y_i\}_{i=1}^M$. We then use those noisy quantile estimates for calibration, at the expense of a small amount of bias.

More precisely, assuming that the estimator \hat{x} is differentiable almost everywhere, the SURE estimate of (4) is given by

$$\text{SURE}(y) = \frac{1}{m} \|y - A\hat{x}(y)\|_2^2 - \sigma^2 + \frac{2\sigma^2}{m} \text{div}(A\hat{x}(y)), \tag{5}$$

where $\text{div}(\cdot)$ denotes the divergence operator [12]. It is easy to show that $\text{SURE}(Y)$ provides an estimate of $s(X, Y)$ that is unbiased [12]. Crucially, when $m = \text{dim}(y)$ is large, the estimate provided by SURE is not only unbiased but also often very accurate (see [12, 13] for a theoretical analysis of the variance of SURE and [14] for an empirical analysis in an imaging setting). As a consequence, we expect that the conformal calibration quantiles obtained from SURE will be in close agreement with the true quantiles of $s(X, Y)$, ensuring that the resulting conformal prediction sets nearly maintain their desired coverage properties.

With regards to the evaluation of SURE, for some model-based estimators it is possible to identify a closed-form expression [15]. Otherwise, computing SURE requires a numerical approximation of the divergence term. A common approach is the Monte Carlo SURE (MC-SURE) algorithm [16], which is estimator-agnostic. We use the so-called Hutchinson’s stochastic trace approximation method [17], which is more computationally efficient than MC-SURE and does not require hyper-parameter fine-tuning. More precisely, the divergence $\text{div}(A\hat{x}(y))$ is approximated as follows:

$$\text{div}(A\hat{x}(y)) = \text{trace}(\mathbf{J}_{h(y)}) = \mathbb{E}[\tilde{n}^\top \mathbf{J}_{h(y)} \tilde{n}], \tag{6}$$

$$\approx \frac{1}{K} \sum_{i=1}^K \tilde{n}_i^\top \mathbf{J}_{h(y)} \tilde{n}_i, \tag{7}$$

$$\approx \frac{1}{K} \tilde{n}^\top \mathbf{J}_{\tilde{n}^\top h(y)}, \tag{8}$$

where $\{\tilde{n}_i\}_{i=1}^K$ are a K i.i.d. standard normal random vectors, $\mathbf{J}_{h(y)}$ is the Jacobian matrix of the predicted measurements $h(y) = A\hat{x}(y)$ with respect to y , and (7) corresponds to Hutchinson’s method, which for computational efficiency we implement (8) using automatic differentiation, as suggested in [17]. This allows obtaining accurate SURE estimates in a highly efficient manner, even in very large problems.

Adopting a split-conformal strategy, after computing $\hat{x}(y_i)$ and $\text{SURE}(y_i)$, for each $i = \{1, \dots, M\}$ we construct the $(1 - \alpha)$ -prediction set $\hat{C}(y_i)$ as:

$$\hat{C}(y_i) = \{x \in \mathbb{R}^n : \|Ax - A\hat{x}(y_i)\|_2^2/m \leq \hat{Q}_\alpha^{(i)}\},$$

where $\hat{Q}_\alpha^{(i)}$ is the top $\frac{\lceil M(1-\alpha) \rceil}{M-1}$ -quantile of the sample $\{\text{SURE}(y_j)\}_{j=1}^M$ with the i th element, $\text{SURE}(y_i)$, removed. Note that while the proposed approach has some bias due to the estimation error introduced by SURE, in our experience the bias is small and arguably significantly smaller than the bias that is likely to be incurred due to distribution shift in deployment. It is also worth mentioning that the estimates $\text{SURE}(y_i)$ can be computed in parallel. The proposed method is summarised in Algorithm 1 below.

Algorithm 1 SURE-based conformal prediction

Input: Forward operator A , noise variance σ^2 , estimator \hat{x} , measurement y , samples $\{y_i\}_{i=1}^M$, precision level $1 - \alpha \in (0, 1)$.

- 1: **for** $i \leftarrow 1$ to M **do**
- 2: $S_i \leftarrow \text{SURE}(y_i)$ using (5) and (8)
- 3: **end for**
- 4: $\hat{Q}_\alpha \leftarrow$ top $\frac{\lceil (M+1)(1-\alpha) \rceil}{M}$ -quantile of $\{S_i\}_{i=1}^M$
- 5: $m \leftarrow \text{dim}(y)$
- 6: $\hat{C}(y) \leftarrow \{x \in \mathbb{R}^n \mid \|Ax - A\hat{x}(y)\|_2^2/m \leq \hat{Q}_\alpha\}$

Output: Prediction set $\hat{C}(y)$

4 Experiments

We demonstrate the proposed self-supervised conformal prediction approach by applying it to two image restoration problems: image denoising and image deblurring. To showcase the versatility of the method, for image denoising we construct conformal prediction sets by using a learning-based image restoration technique trained in a self-supervised end-to-end manner, whereas for image deblurring we use the model-driven technique. For each experiment, we implement our method by using Algorithm 1 to compute conformal prediction sets. We consider a fine grid of values for the confidence parameter $\alpha \in (0, 1)$, ranging from 0% to 100%. The corresponding prediction sets should cover the solution

space with a probability of approximately $1 - \alpha$. We evaluate the accuracy of these prediction sets by calculating the empirical coverage probabilities on a test set. Specifically, we compute the proportion of test images that lie within the conformal prediction sets for various confidence levels. In all experiments, the calibration sample size M is chosen to be sufficiently large to ensure that the variability of the sample quantiles caused by the finite-sample correction is negligible. Furthermore, for comparison, in each experiment we also report results by supervised conformal prediction (i.e., using ground truth data for calibration, rather than SURE). The experiments are implemented using the Deep Inverse library⁴ for imaging with deep learning using PyTorch.

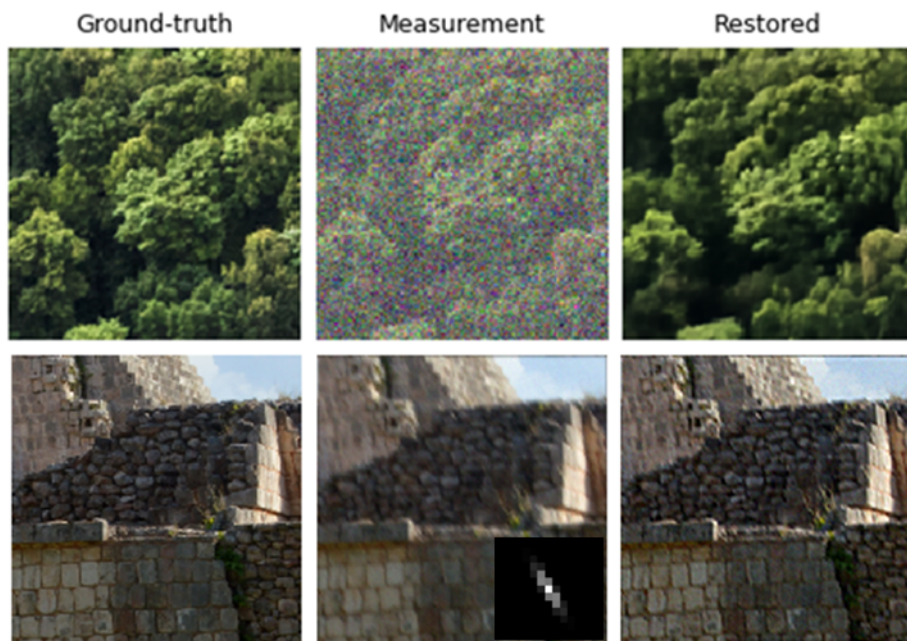


Fig. 1: **Image reconstruction results for various imaging problems.** Top: Gaussian noise on DIV2K. Bottom: Noisy Gaussian blur on DIV2K

4.1 Image Denoising

For the image denoising experiment, we consider colour images of size 128×128 pixels obtained by cropping images from the DIV2K dataset [18], which we artificially degrade by adding white Gaussian noise with a standard deviation of $\sigma = 0.1$. As image restoration method, we use a DRUNet model [19] trained in a

⁴ <https://deepinv.github.io/deepinv/>

self-supervised manner by using the SURE loss [20]. The training data consists of 900 noisy measurements, we do not use any form of ground truth for training or for conformal prediction. See the top row of Fig. 1 for an example of a clean image, its noisy measurement, and the estimated reconstruction. We then use these same noisy images to compute our proposed self-supervised conformal prediction sets, and assess their accuracy empirically by using 200 measurement-truth pairs from the test dataset. The results are reported in Fig. 2 below, together with the results obtained by using the equivalent supervised conformal prediction approach that relies on ground truth data for calibration. We observe that our method delivers prediction sets that are remarkably accurate and in close agreement with the results obtained by using supervised conformal prediction, demonstrating that the bias stemming from using SURE instead of ground truth data is negligible in this case. For completeness, Fig. 4 (left) below shows the empirical distribution of the non-similarity function $s(x, y)$ for the supervised conformal prediction based on the MSE, and the proposed self-supervised conformal prediction based on a SURE estimate of the MSE. Again, we observe close agreement between these distributions, with the SURE distribution being slightly more spread due to the random error inherent to SURE.

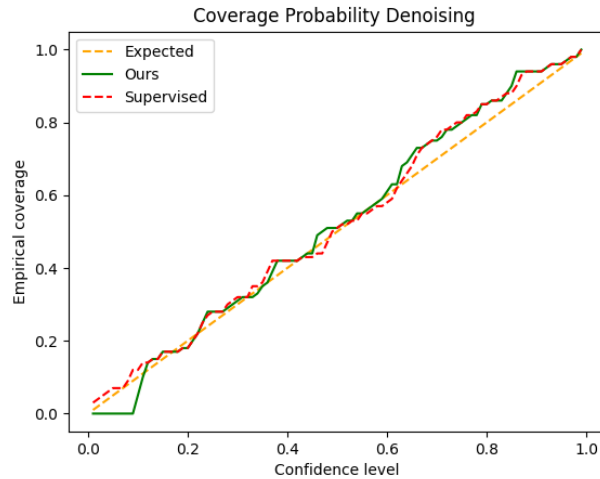


Fig. 2: **Image denoising experiment:** desired confidence level vs empirical coverage. Both supervised and the proposed self-supervised conformal prediction methods deliver prediction sets with near perfect coverage.

4.2 Image Deblurring

We now consider a non-blind image deblurring experiment with colour images of size 256×256 pixels, derived from the DIV2K dataset [18] and artificially degraded with a diagonal Gaussian blur of major bandwidth $\varsigma_0 = 2$, $\varsigma_1 = 0.3$ along the minor axis, and an inclination of $\pi/6$ degrees, as well as additive white Gaussian noise with a standard deviation $\sigma = 0.01$. As image restoration technique, we use the recently proposed model-based Polyblur technique [21], a highly efficient restoration method for removing mild blur from natural images based on a truncated polynomial approximation of the inverse of the blur kernel. See the bottom row of Fig. 1 for an example of a clean image, its noisy measurement, and the estimated reconstruction.

We use 900 blurred and noisy images to compute our proposed self-supervised conformal prediction sets, and assess their accuracy empirically by using 200 measurement-truth pairs from the test dataset. The results are reported in Fig. 3 below, together with the results obtained by using the equivalent supervised conformal prediction approach that relies on ground truth data for calibration. Again, we observe that our method delivers prediction sets that are accurate and remarkably close to the results obtained by using supervised conformal prediction, demonstrating that the bias stemming from using SURE instead of ground truth data is again negligible in this case. For completeness, Fig. 4 (right) below shows the empirical distribution of the non-similarity function $s(x, y)$ for the supervised conformal prediction based on the MSE, and the proposed self-supervised conformal prediction based on a SURE estimate of the MSE. Again, we observe close agreement between these distributions.

5 Discussion and Conclusion

This paper presented a self-supervised approach for constructing conformal prediction regions for linear imaging inverse problems that are ill-posed. Unlike previous conformal prediction methods, the proposed approach does not require any form of ground truth data. This is achieved by leveraging Stein’s unbiased risk estimator and by pooling together a group of exchangeable imaging problems. This allows delivering conformal prediction sets in situations where there is no ground truth data available for calibration, and provides robustness to distribution shift. Additionally, the proposed framework is estimator-agnostic, as it uses a Monte Carlo implementation of SURE that does not require any explicit knowledge of the image restoration algorithm used. This flexibility allows the framework to be straightforwardly applied to model-driven as well as data-driven image restoration techniques, including self-supervised data-driven techniques that are also trained directly from the measurement data. Moreover, the method is computationally efficient as computations can be performed in parallel. We demonstrated the effectiveness of the proposed method through image denoising and deblurring experiments, where we observed that our method delivers extremely accurate prediction sets.

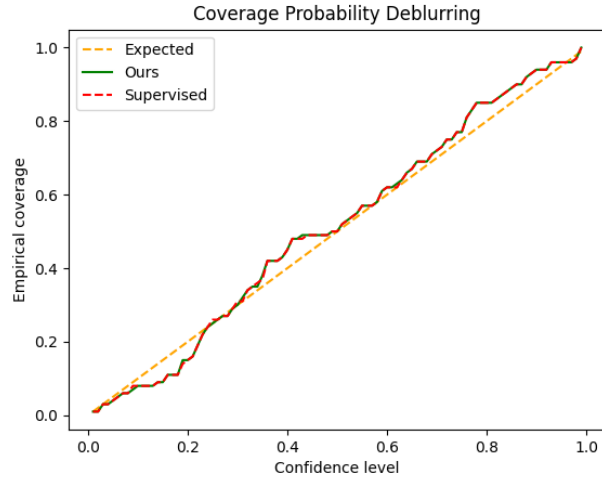


Fig. 3: **Image deblurring experiment**: desired confidence level vs empirical coverage. Both supervised and the proposed self-supervised conformal prediction methods deliver prediction sets with near perfect coverage.

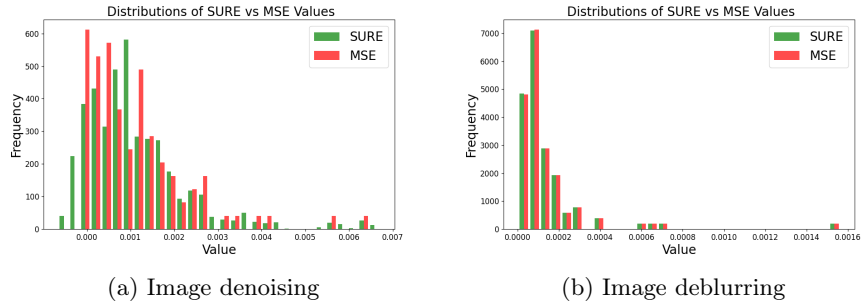


Fig. 4: **Calibration histograms** (empirical distribution of the non-similarity function $s(x, y)$) for the supervised case (MSE) and the self-supervised case based on a SURE estimate of the MSE, for the denoising and deblurring experiments.

Future work will explore the generalization of the proposed approach to other noise models, such as Poisson and Poisson-Gaussian, as well as to problems in which the parameters of the noise model are unknown [20]. Another important perspective for future work is to extend this approach to problems in which the forward A is not full rank, for example by leveraging equivariance properties. In particular, it would be interesting to study the integration of our proposed method and the equivariant bootstrap [7].

Bibliography

- [1] J. Kaipio and E. Somersalo, *Statistical and computational inverse problems*. Germany: Springer, 2004.
- [2] A. Durmus, E. Moulines, and M. Pereyra, “Efficient bayesian computation by proximal markov chain monte carlo: When langevin meets moreau,” *SIAM Journal on Imaging Sciences*, vol. 11, no. 1, pp. 473–506, 2018.
- [3] M. Pereyra, “Maximum-a-posteriori estimation with bayesian confidence regions,” *SIAM Journal on Imaging Sciences*, vol. 10, no. 1, pp. 285–302, 2017.
- [4] R. Laumont, V. D. Bortoli, A. Almansa, J. Delon, A. Durmus, and M. Pereyra, “Bayesian imaging using plug & play priors: when langevin meets tweedie,” *SIAM Journal on Imaging Sciences*, vol. 15, no. 2, pp. 701–737, 2022.
- [5] M. Holden, M. Pereyra, and K. C. Zygalakis, “Bayesian imaging with data-driven priors encoded by neural networks,” *SIAM Journal on Imaging Sciences*, vol. 15, no. 2, pp. 892–924, 2022.
- [6] D. Y. W. Thong, C. K. Mbakam, and M. Pereyra, “Do bayesian imaging methods report trustworthy probabilities?” 2024. [Online]. Available: <https://arxiv.org/abs/2405.08179>
- [7] J. Tachella and M. Pereyra, “Equivariant bootstrapping for uncertainty quantification in imaging inverse problems,” *Proceedings of Machine Learning Research*, vol. 238, pp. 4141–4149, 2024.
- [8] M. Cherif, T. I. Liaudat, J. Kern, C. Kervazo, and J. Bobin, “Uncertainty quantification for fast reconstruction methods using augmented equivariant bootstrap: Application to radio interferometry,” 2024. [Online]. Available: <https://arxiv.org/abs/2410.23178>
- [9] A. N. Angelopoulos and S. Bates, “A gentle introduction to conformal prediction and distribution-free uncertainty quantification,” *arXiv preprint arXiv:2107.07511*, 2021.
- [10] D. Narnhofer, A. Habring, M. Holler, and T. Pock, “Posterior-variance-based error quantification for inverse problems in imaging,” *SIAM Journal on Imaging Sciences*, vol. 17, no. 1, pp. 301–333, 2024.
- [11] C. Johnstone and B. Cox, “Conformal uncertainty sets for robust optimization,” in *Conformal and Probabilistic Prediction and Applications*. PMLR, 2021, pp. 72–90.
- [12] C. M. Stein, “Estimation of the mean of a multivariate normal distribution,” *The annals of Statistics*, pp. 1135–1151, 1981.
- [13] P. C. Bellec and C.-H. Zhang, “Second-order stein: Sure for sure and other applications in high-dimensional inference,” *The Annals of Statistics*, vol. 49, no. 4, pp. 1864–1903, 2021.
- [14] E. J. Candès, C. A. Sing-Long, and J. D. Trzasko, “Unbiased risk estimates for singular value thresholding and spectral estimators,” *IEEE Transactions on Signal Processing*, vol. 61, no. 19, pp. 4643–4657, 2013.

- [15] R. J. Tibshirani and J. Taylor, “Degrees of freedom in lasso problems,” *The Annals of Statistics*, vol. 40, no. 2, pp. 1198–1232, 2012.
- [16] S. Ramani, T. Blu, and M. Unser, “Monte-Carlo SURE: A black-box optimization of regularization parameters for general denoising algorithms,” *IEEE Transactions on image processing*, vol. 17, no. 9, pp. 1540–1554, 2008.
- [17] S. Soltanayev, R. Giryes, S. Y. Chun, and Y. C. Eldar, “On divergence approximations for unsupervised training of deep denoisers based on stein’s unbiased risk estimator,” in *ICASSP 2020 - 2020 IEEE International Conference on Acoustics, Speech and Signal Processing (ICASSP)*, 2020, pp. 3592–3596.
- [18] E. Agustsson and R. Timofte, “Ntire 2017 challenge on single image super-resolution: Dataset and study,” in *The IEEE Conference on Computer Vision and Pattern Recognition (CVPR) Workshops*, July 2017.
- [19] K. Zhang, Y. Li, W. Zuo, L. Zhang, L. Van Gool, and R. Timofte, “Plug-and-play image restoration with deep denoiser prior,” *IEEE Transactions on Pattern Analysis and Machine Intelligence*, vol. 44, no. 10, pp. 6360–6376, 2021.
- [20] J. Tachella, M. Davies, and L. Jacques, “Unsure: Unknown noise level stein’s unbiased risk estimator,” *arXiv preprint arXiv:2409.01985*, 2024.
- [21] M. Delbraccio, I. Garcia-Dorado, S. Choi, D. Kelly, and P. Milanfar, “Poly-blur: Removing mild blur by polynomial reblurring,” *IEEE Transactions on Computational Imaging*, vol. 7, pp. 837–848, 2021.